ELSEVIER

International Journal of Adhesion & Adhesives 28 (2008) 329–339

International Journal of Adhesion & Adhesives

www.elsevier.com/locate/ijadhadh

High strain-rate compression and tension behaviour of an epoxy bi-component adhesive

L. Goglio*, L. Peroni, M. Peroni, M. Rossetto

Dipartimento di Meccanica, Politecnico di Torino, Corso Duca Degli Abruzzi 24, 10129 Torino, Italy

Accepted 9 August 2007
Available online 6 November 2007

Abstract

The dynamic behaviour of the bonded joints is influenced by the dynamic mechanical properties of the material of adherends and adhesives. The literature contains plenty of information about the dynamic mechanical properties of many structural materials (especially metals), obtained through different test types. Conversely, the study of the dynamic mechanical properties of the adhesives is not so common. The purpose of this work is to assess the dynamic mechanical behaviour of an epoxy bi-component adhesive for structural bonding. In particular, the study has been focussed on the influence of the strain-rate on the tensile and compressive strength of specimens made of adhesive. The experimental tests have been performed with a hydraulic universal testing machine and a tensile-compression Hopkinson bar. The results of the tests show that the adhesive strength increases substantially by increasing the strain-rate. The Cowper–Symonds and Johnson–Cook models of strain-rate dependence have been used to fit the experimental data with unsatisfactory results, thus also a poly-linear fit has been adopted.

Keywords: Epoxies; Mechanical properties of adhesives; Impact; Strain-rate; Hopkinson bar

1. Introduction

In many structural and mechanical applications, the applied loads can be dynamic or even impulsive. Bonded-joint technology is frequently used in industrial sectors where impact and bump are very common, as the automotive sector. From this viewpoint, the design requires the knowledge of the high strain-rate mechanical behaviour of the used materials. In literature, most studies concern the dynamic behaviour of metals and other structural materials, while only a few concern adhesives [1–3]. The purpose of this paper is to study the impact behaviour of an epoxy bi-component adhesive for structural applications. In detail, the attention is focussed on the study of the stress–strain curves of specimens made entirely in adhesive, to avoid the influence of the adherends and joint geometry on the results. The experimental tests have been designed to investigate the influence of the strain-rate on the strength of material in a large range, from 1×10^{-3} to $3 \times 10^{3}\,s^{-1}$. Such a large range has been chosen to verify the applicability of the Cowper–Symonds and the Johnson–Cook models [4,5] (generally applied to metals) to an adhesive. The experimental plan also considers the influence of different curing conditions (at room temperature and at 100 °C) on the mechanical behaviour of the adhesive.

2. Experimental set-up

For the very large range of considered strain-rate, it is impossible to perform all tests with the same equipment. Therefore, two equipments have been used:

- a universal servo-hydraulic test machine for tests at strain-rate lower than $12\,s^{-1}$;
- a split Hopkinson pressure bar (SHPB) for tests at up to $3.0 \times 10^{3}\,s^{-1}$.

Both equipments, situated in the La.Di.Spe. Laboratory of the Vercelli site of the Politecnico di Torino, are used for tensile and compression tests. In the next paragraph, the

*Corresponding author. Tel.: +39 011 5646934; fax: +39 011 5646999.
E-mail address: luca.goglio@polito.it (L. Goglio).

0143-7496/$ - see front matter © 2007 Elsevier Ltd. All rights reserved.
doi:10.1016/j.ijadhadh.2007.08.004

description of the servo-hydraulic machine is omitted (for its very large diffusion) and a short introduction about SHPB is given.

No experimental test has been performed in the range 10^1–$10^2\,s^{-1}$, since the above-mentioned equipments are not suitable for it. In the case of the servo-hydraulic machine, there are limitations due to maximum crosshead speed and inertial effects on the force and displacement transducer. In the case of the SHPB, the limitation is due to the specimen size, as explained in the next paragraph. This strain-rate range could be covered by falling weight equipments, but in this case the difficulty would affect the accuracy in measuring stress and strain in the specimen.

2.1. Split Hopkinson pressure bar

SHPB is the main testing device to investigate the dynamic behaviour of the materials at medium-high strain-rate (1×10^3 to $5\times10^3\,s^{-1}$). At first SHPB was used only for compression tests on metals [6], but in the last years many studies proposed different set-ups for tension, torsion and bending tests on different kinds of material like polymers, foams, ceramics, etc. [7–11]. In the following, the compression and tension configurations for the equipment used in the present work are presented.

2.1.1. Compression test configuration

The standard configuration of the SHPB performs dynamic compression tests, usually on cylindrical specimens. Fig. 1 shows the sketch of a simplified compression SHPB and the related Lagrangian diagram. The test starts when the impact of the striker rod against the input bar generates an ideally rectangular compression pulse. The pulse propagates along the input bar, reaches the specimen and is partially reflected and partially propagates through the specimen and the output bar. By measuring the reflected pulse on the input bar and the transmitted pulse on the output bar, it is possible to reconstruct the dynamic stress–strain curve of the tested material by means of the following equations [6]:

$$\sigma_{\text{specimen}}(t) = E_0\frac{A_0}{A}\varepsilon_{\text{transmitted}}(t), \tag{1}$$

$$\varepsilon_{\text{specimen}}(t) = -\frac{2c_0}{L}\int \varepsilon_{\text{reflected}}(t)\,dt, \tag{2}$$

$$\dot{\varepsilon}_{\text{specimen}}(t) = -\frac{2c_0}{L}\varepsilon_{\text{reflected}}(t), \tag{3}$$

where A and L are, respectively, cross-section and length of the specimen; A_0, c_0 and E_0 are cross-section, wave velocity and elastic modulus of the bars. The measurement is carried out by means of strain gauges applied on the bars (see Fig. 1), with the advantage that it is not required to place sensors on the specimen. It is clear from Eq. (3) that different strain-rate values can be achieved by varying the specimen length or the deformation amplitude. In the ideal case of rectangular reflected pulse, the specimen would deform at constant strain-rate during the impact, in practice the strain-rate is not constant [12] and a mean value over the impact is taken, after that the measurement has been completed.

There are also some practical constraints about the size of specimen tested with an SHPB and consequently on the obtainable strain-rate. In fact Eqs. (1)–(3) are obtained under the fundamental hypothesis of uniform stress–strain field in the specimen that is only reached if the specimen length is much smaller than the length of the pulse. In practice, for this reason, the minimum strain-rate obtainable with a standard SHPB is about $5.0\times10^2\,s^{-1}$.

Moreover, Eqs. (1)–(3)—which are obtained by the mono-dimensional theory of elastic wave propagation (the rods are thin and they remain in linear elastic conditions)—do not consider the dispersion phenomena due to the lateral contraction. Therefore, before applying these equations, the measurements have been treated by means of the technique described in Ref. [13] that allows for compensating signal distortion.

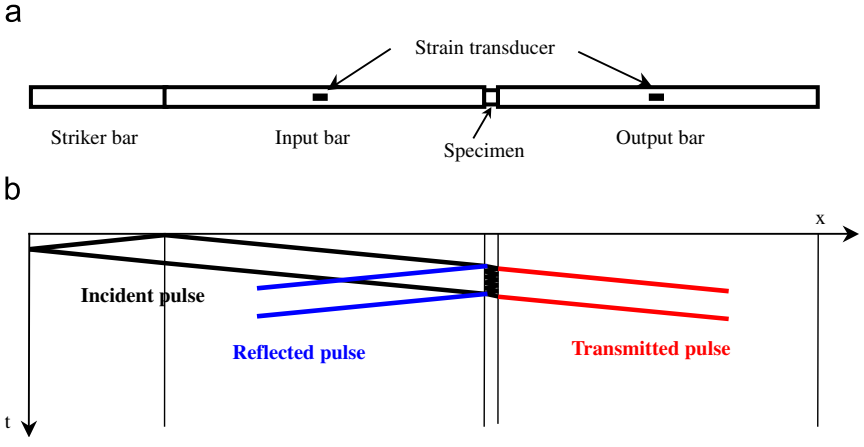

Fig. 1. Schematics of the equipment (a) and Lagrangian diagram (b).

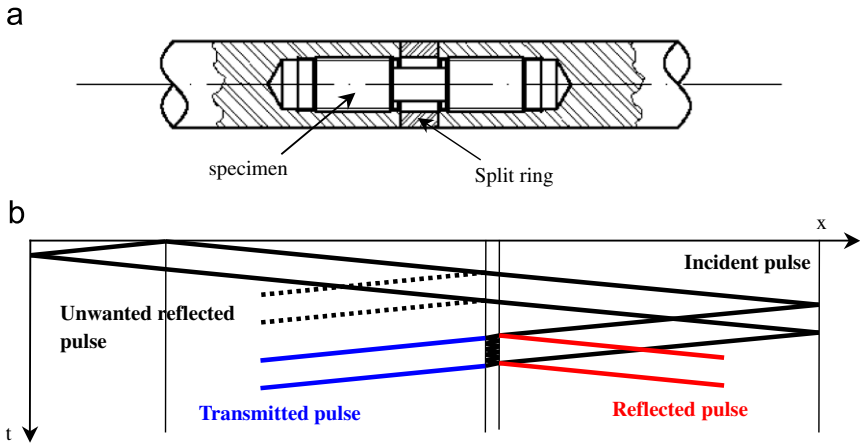

Fig. 2. Tensile specimen holding device and split ring (a) and Lagrangian diagram (b).

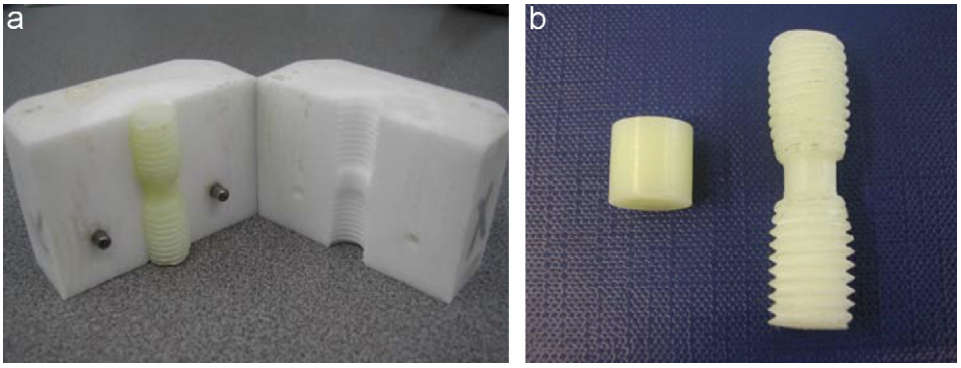

Fig. 3. Mould for tensile specimens (a) and example of compression and tensile specimen (b).

2.1.2. Tensile test configuration

The greatest difficulty in tensile SHPB test is the generation of the tensile elastic pulse in the incident bar. Since the adopted striker system is the same as for the compression tests, the tensile pulse is created by means of a "reflection system" [7,11,12]. The specimen has the classical hourglass shape used for static tests, with two threaded extremities that are directly screwed in the bars (which have one threaded hole at the extremity). A split ring of the same length of the calibrated zone of the specimen is placed around the specimen. Fig. 2 shows the specimen clamping system with the split ring and the related Lagrangian diagram.

The split ring transmits the first compression pulse from the first to the second bar (since the specimen is much more compliant than the ring, the stress in the specimen is negligible). When the compression pulse reaches the free end of the second bar, it is reflected as a tensile pulse. Thus, the second bar becomes the input bar and the first bar becomes the output bar. The tensile pulse is transmitted from one bar to the other only by the specimen, since the split ring does not transmit the tension. In addition to this, it must be also considered that when the first compression pulse reaches the split ring also an unwanted reflection in the first bar occurs. This generates a pulse travelling back and forth through the first bar that may interfere with the tensile pulse transmitted through the specimen. For this reason, the sensor positions must be accurately chosen to avoid superposition of undesired reflections on interesting signals [7,14,15].

3. Specimens

The adhesive considered in this work is the Henkel Loctite Hysol 9466, a bi-component epoxy for structural bonded joints. The main properties given by the technical datasheet for the adhesive cured at room temperature are: glass transition temperature 62 °C, elongation 3%, tensile strength 32 MPa, tensile modulus 1718 MPa (mechanical properties according to ISO 527-3). Cured at room temperature this adhesive already develops its full strength after 24 h; at 100 °C this time reduces to about half an hour. To investigate the possible effects of the curing temperature on the mechanical properties, two test series have been carried out, one with cold cured adhesive (room temperature) and the other with hot cured adhesive (100 °C). Both series have been tested in compression and in tension. All specimens have been made by pouring the adhesive in Teflon moulds properly shaped. Teflon is essential to avoid that specimen remain bonded to the mould and does not

need lubricant that could react with the adhesive altering its mechanical properties. Fig. 3 shows the mould for tensile specimens and an example of compression and tensile specimen.

The compression specimens for static and dynamic tests have cylindrical shape with a diameter of 10 mm. The length values adopted to obtain the desired nominal strain-rate on SHPB are about 4 mm (nominal strain-rate $3.0 \times 10^3\,s^{-1}$), 7 mm ($2.0 \times 10^3\,s^{-1}$), 10 mm ($1.5 \times 10^3\,s^{-1}$). Note that the strain-rate is not simply proportional to the inverse of the specimen length because according to Eq. (3) it depends also on the reflected signal $\varepsilon_{reflected}(t)$ (and therefore on the intensity of the impact). The actual strain-rate can be assessed only after the test by processing the measurements. For the tests carried out on the hydraulic machine—on which, by changing the crosshead speed, the strain-rate (equal to the ratio of the speed to the length) can be adjusted—the adopted length values are 10 mm for strain-rate up to $0.5 \times 10^1\,s^{-1}$ and 4 mm in the case $1.2 \times 10^1\,s^{-1}$.

The tensile test specimens for static and dynamic tests have cylindrical geometry with two threaded ends M10. The diameter of the constant cross-section is 6 mm, while the length of this zone is 5 mm. On SHPB, different strain-rates are obtained by varying the velocity of the

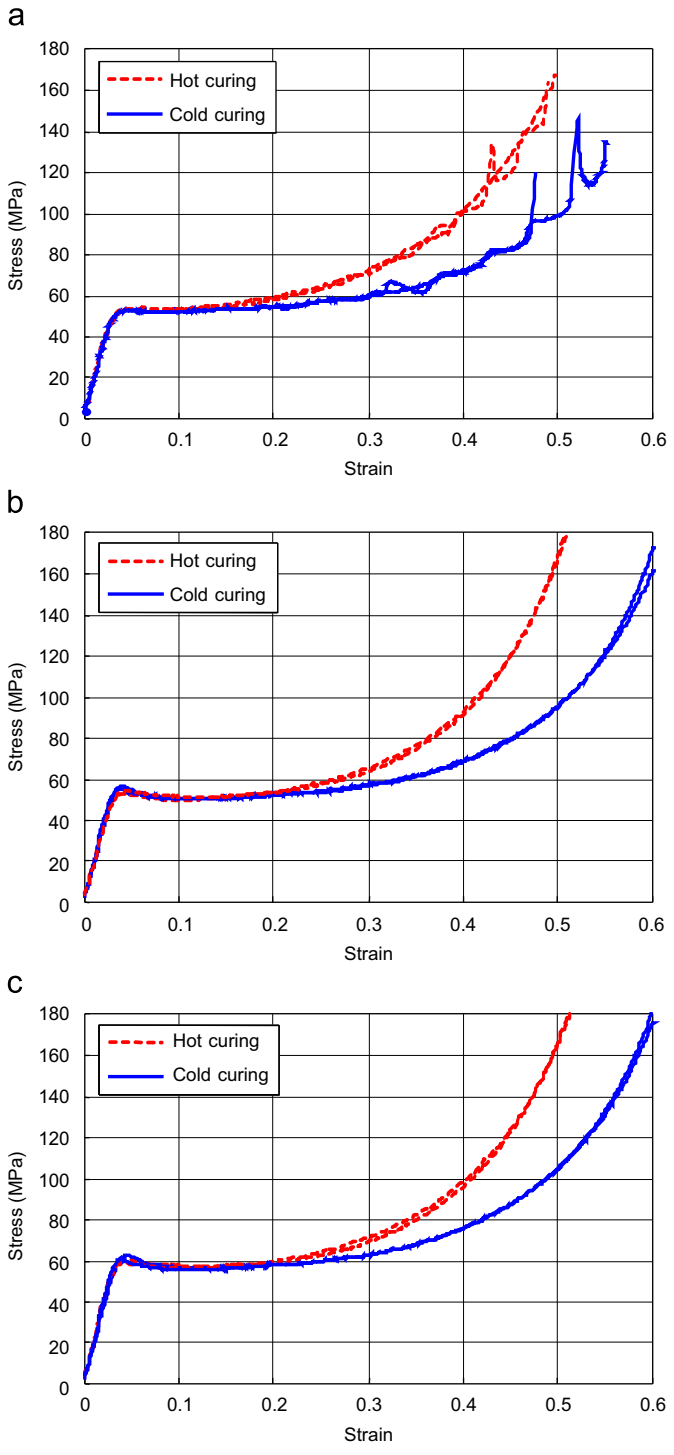

Fig. 4. Comparison of the compression static tests at $10^{-3}\,s^{-1}$ (a), $10^{-2}\,s^{-1}$ (b), $10^{-1}\,s^{-1}$ (c) for hot and cold curing.

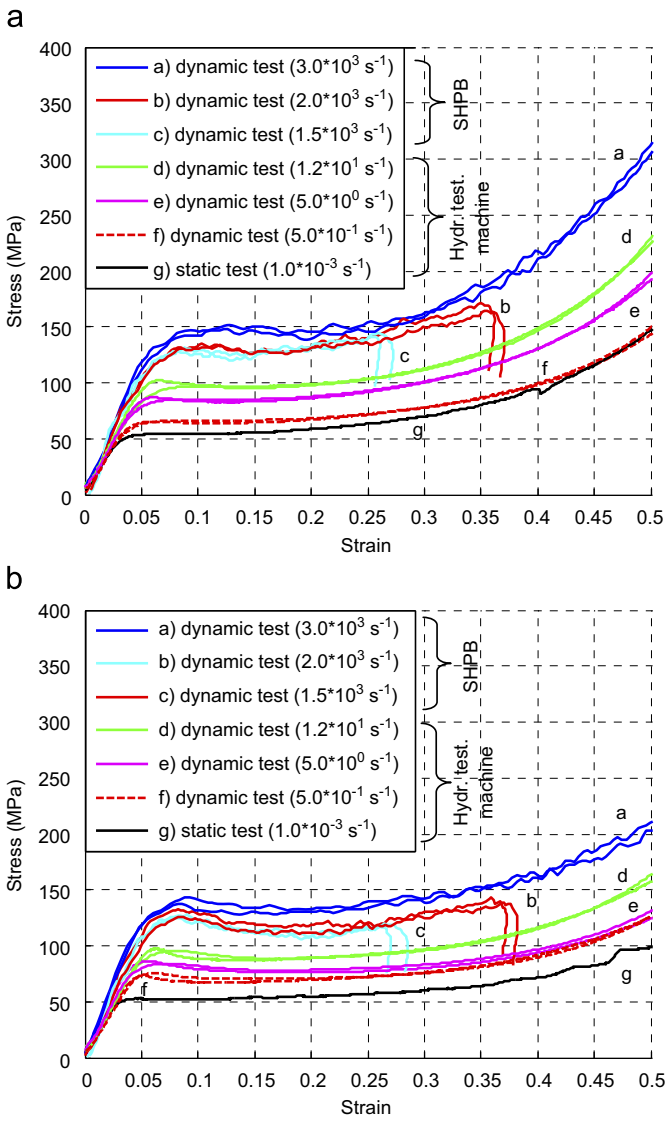

Fig. 5. Summary of the compression tests on specimens: (a) hot cured and (b) cold cured.

striker bar. This allowed for avoiding the manufacture of different moulds.

The curing procedures followed for both compression and tension specimens are:

- *cold curing*: adhesive cured for 24 h at room temperature in the Teflon mould;
- *hot curing*: adhesive cured in a oven at 100 °C for 30 min and cooled at room temperature.

In both cases, the specimens have been aged for a week at room temperature before testing.

4. Results and discussion

4.1. Compression tests

4.1.1. Compression static tests

As the tests performed at strain-rate up to $10^{-1}\,s^{-1}$ are referred to as static, such assumption is justified by the observed behaviour of the material (see k factor at the end of Section 4.1.2). In Fig. 4 the comparison of the test results is proposed, in terms of engineering stress–strain curves, for the two different types of curing and all strain-rate values (two replications have been carried out for each case). It can be observed that the two different kinds of curing give the same elastic properties (elastic modulus E and proof stress $R_{p0.2}$). Only in the plastic range of the curves, there are some differences; in particular hot curing shows higher strain-hardening than cold curing. The oscillations of the stress–strain curves in the plastic range are due to stick-slip phenomena that take place even if the faces of the specimen have been lubricated with oil immediately before the tests. It can be also appreciated from Fig. 4 that these levels of strain-rate have little influence on the behaviour of the material; this confirms the assumption of treating these cases as static.

4.1.2. Compression dynamic test

As stated previously, the dynamic compression tests have been performed with the universal servo-hydraulic machine Dartec HA 100 for strain-rate values up to $1.2 \times 10^{1}\,s^{-1}$. A gap between crosshead and specimen is left at the beginning of the test, so that the crosshead can reach the required speed before the compression begins. The tests at higher strain-rates have been performed with the SHPB and are identified by their nominal values.

Fig. 5 shows, superposed in the same diagram separately for hot and cold curing, the stress–strain curves for the static test at $10^{-3}\,s^{-1}$ (mean curve over the replications) and for all dynamic tests (two replications for each case). The progressive rise of the curves as the strain-rate increases can be appreciated. The shorter extension of the curves corresponding to nominal strain-rate 1.5×10^{3} and $2.0 \times 10^{3}\,s^{-1}$ is due to the fact that being equal the displacement applied by the bar to the specimen end, the longer the specimen, the lower the total strain.

It can be noticed that the dynamic stress–strain curves present almost the same shape as the static ones, and the hot curing curves exhibit higher strain-hardening than the cold curing curves, for all strain-rate levels.

Table 1 reports—separately for hot and cold curing—the values of nominal and actual mean strain-rate, the corresponding obtained elastic modulus and 0.2% proof

Table 1
Summary of the compression tests results: (a) hot curing and (b) cold curing

	$\dot{\varepsilon}_{nominal}$ (s^{-1})	$\dot{\varepsilon}_{actual,mean}$ (s^{-1})	E (GPa)	$R_{p0.2}$ (MPa)
(a) Hot curing				
Static tests	1.0×10^{-3}	$1.00 \times 10^{-3}/1.00 \times 10^{-3}$	1.98/1.97	48/48
	1.0×10^{-2}	$1.30 \times 10^{-2}/1.20 \times 10^{-2}$	1.92/2.00	51/52
	1.0×10^{-1}	$1.14 \times 10^{-1}/1.12 \times 10^{-1}$	1.93/1.98	59/60
Dynamic tests (hydraulic machine)	5.0×10^{-1}	$5.06 \times 10^{-1}/5.32 \times 10^{-1}$	1.99/1.96	67/69
	5.0×10^{0}	$4.95 \times 10^{0}/4.96 \times 10^{0}$	1.96/1.90	83/84
	1.2×10^{1}	$1.23 \times 10^{1}/1.21 \times 10^{1}$	1.95/2.00	95/94
Dynamic tests (SHPB)	1.5×10^{3}	$1.45 \times 10^{3}/1.47 \times 10^{3}$	(2.18/2.30)	127/123
	2.0×10^{3}	$1.96 \times 10^{3}/1.98 \times 10^{3}$	(2.21/2.11)	131/130
	3.0×10^{3}	$3.05 \times 10^{3}/2.99 \times 10^{3}$	(2.42/2.32)	143/144
(b) Cold curing				
Static tests	1.0×10^{-3}	$1.00 \times 10^{-3}/1.00 \times 10^{-3}$	1.98/2.20	47/47
	1.0×10^{-2}	$1.10 \times 10^{-2}/1.00 \times 10^{-2}$	2.00/1.99	52/53
	1.0×10^{-1}	$1.15 \times 10^{-1}/1.13 \times 10^{-1}$	1.92/1.93	60/61
Dynamic tests (hydraulic machine)	5.0×10^{-1}	$5.23 \times 10^{-1}/5.11 \times 10^{-1}$	1.85/1.90	74/75
	5.0×10^{0}	$4.83 \times 10^{0}/4.98 \times 10^{0}$	2.01/2.25	86/86
	1.2×10^{1}	$1.21 \times 10^{1}/1.21 \times 10^{1}$	1.99/1.95	93/95
Dynamic tests (SHPB)	1.5×10^{3}	$1.49 \times 10^{3}/1.48 \times 10^{3}$	(2.17/2.24)	126/122
	2.0×10^{3}	$2.01 \times 10^{3}/2.00 \times 10^{3}$	(2.30/2.09)	131/126
	3.0×10^{3}	$3.04 \times 10^{3}/2.99 \times 10^{3}$	(2.44/2.30)	143/142

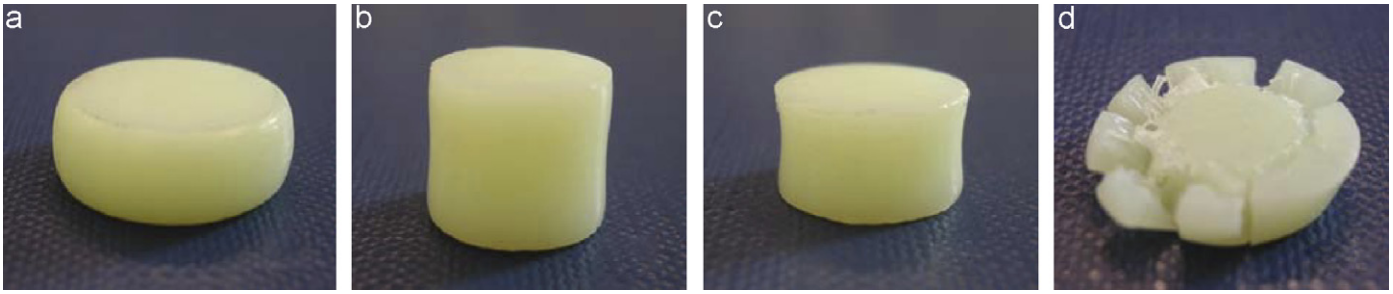

Fig. 6. Specimen comparison: (a) pseudo-static, (b) $1.5 \times 10^3\,s^{-1}$, (c) $2.0 \times 10^3\,s^{-1}$, (d) $3.0 \times 10^3\,s^{-1}$.

stress. Regarding the elastic modulus, it must be remarked that in the tests performed on SHPB, the equilibrium conditions (which are practically reached after the signal has travelled back and forth three times through the specimen [11]) are reached approximately in the same time in which the stress reaches the elastic limit. Therefore, the first part of the stress–strain diagram is affected by this phenomenon and the elastic modulus cannot be evaluated accurately. For this reason, the values are reported in parentheses. However, the values under high strain-rate are in general slightly higher than those obtained statically or at low strain-rate and this is in accordance with the expected trend. Conversely, the elastic limit strongly increases with the strain-rate: at $3.0 \times 10^3\,s^{-1}$ the dynamic values are about three times the values at $1.0 \times 10^{-3}\,s^{-1}$.

Fig. 6 shows four compression specimens tested at different strain-rate values. The specimen subjected to the static loading (Fig. 6a) has the typical deformed shape in which the radial expansion of the central zone is higher than that of the bases because of the friction with the compressing plates (“barrel shape”). The same behaviour occurs for all specimens tested at low strain-rate. The specimens tested at strain-rate $1.5 \times 10^3\,s^{-1}$ and higher, i.e. on the SHPB (Fig. 6b and c) present an unexpected—and, to our knowledge, at the moment not explained—deformed shape in which the radial expansion of the central zone is lower than that of the bases (“hourglass shape”). It can be noted that the deformed shape of the specimen is symmetrical, and this suggests that the phenomenon does not depend on the direction of incident pulse. This feature is almost imperceptible at $1.5 \times 10^3\,s^{-1}$ but becomes very important increasing the strain-rate. Finally, at $3.0 \times 10^3\,s^{-1}$ (Fig. 6d), the specimen collapses and presents several circumferential and radial cracks.

To help the analysis of the plastic behaviour, the stress–strain curves are reported as in Fig. 7, in which each curve is started at the beginning of the plateau and is shifted horizontally to set the initial strain equal to zero (i.e. the abscissa is the total strain after yield). The observation of these diagrams suggests that the curve corresponding to a generic strain-rate value can be obtained from the static curve scaled by a dynamic factor $k = \sigma_{dynamic}/\sigma_{static}$, function of the strain-rate. The theoretical background for this operation can be found in the models that account for the strain-rate dependency

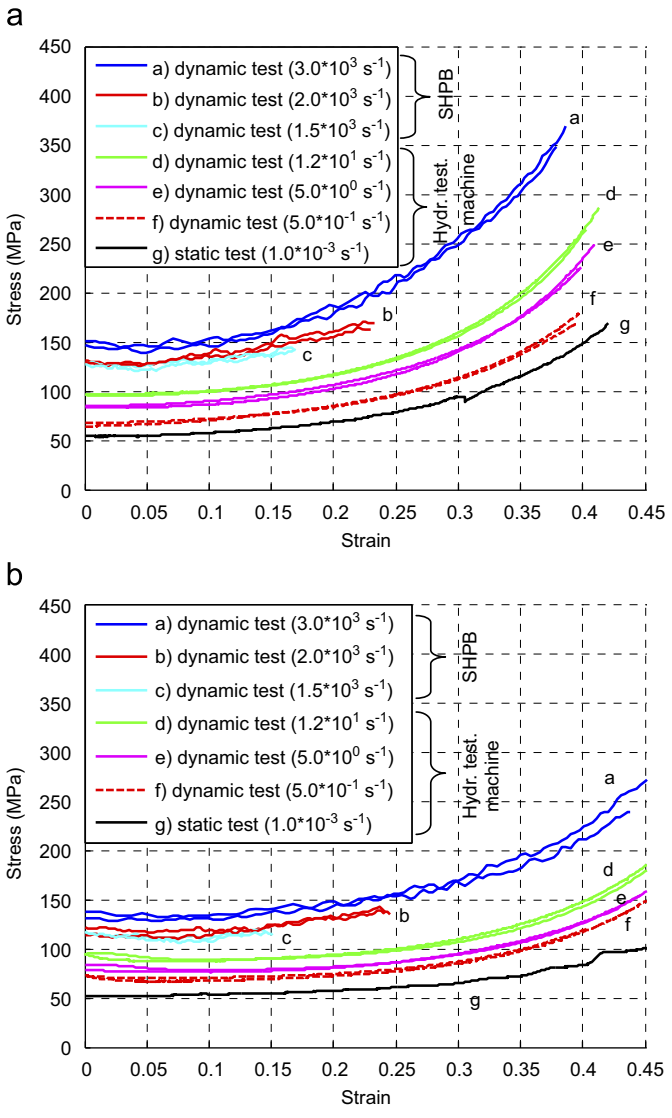

Fig. 7. Comparison of the dynamic stress–strain curves after the elastic range: (a) hot curing and (b) cold curing.

(originally applied to metals), such as the Cowper–Symonds and Johnson–Cook models [4,5]. The former is expressed by the equation:

$$k = 1 + \left(\frac{\dot{\varepsilon}}{D}\right)^{1/q}, \tag{4}$$

where D and q are the two parameters of the model, $\dot{\varepsilon}$ is the strain-rate and k is the dynamic scale factor. The Johnson–Cook model, ignoring thermal influences (not involved in our cases), has the form:

$$k = 1 + C \ln \frac{\dot{\varepsilon}}{\dot{\varepsilon}_0}, \tag{5}$$

where the two parameters of the model are in this case the multiplier C and the strain-rate $\dot{\varepsilon}_0$, threshold at which the dynamic effects become influent, while $\dot{\varepsilon}$ and k have the same meaning as in the previous model.

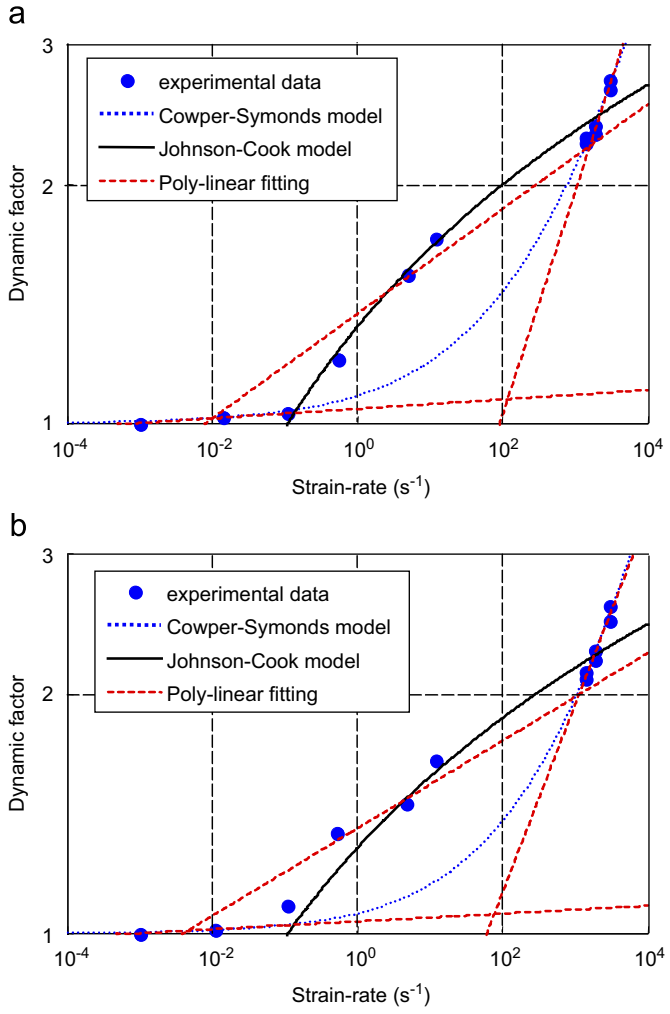

Fig. 8. Dynamic scale factor for specimens: (a) hot cured and (b) cold cured.

The experimental determination of the dynamic factor k has been achieved by minimising the deviation of the dynamic curve from the model, i.e. the static curve scaled by k, with a least square algorithm applied to the whole curve (the static curve taken as reference, as in Fig. 7, is the average of the two tests at $10^{-3}\,s^{-1}$). This procedure is more robust than simply considering the ratio of the dynamic stress to the static stress for a single point (like yield stress or $R_{p0.2}$), as usually done [4].

Fig. 8 shows, separately for the cases of hot and cold curing, the k factor as a function of the actual strain-rate. All of the tests are presented, the experimental points seem to be less than the tests reported in Table 1 because at strain-rate under $10^2\,s^{-1}$ the two replications are almost perfectly coincident. Each diagram contains, besides the experimental points, the curves—obtained by least squares fitting—corresponding to the two above-mentioned models. The Cowper–Symonds model interpolates correctly the experimental data at the two extremities of the strain-rate range but fails to reproduce the intermediate values. On the contrary, the Johnson–Cook model fits better the points at intermediate values, gives a less accurate approximation of the points at high strain-rate and fails to reproduce the behaviour at low strain-rate. In addition to these models, a simple poly-linear fitting has been applied. The latter is composed of two or more linear segments (in a log–log scale) in the form $k = A\dot{\varepsilon}^m$, where A and m are the fitting

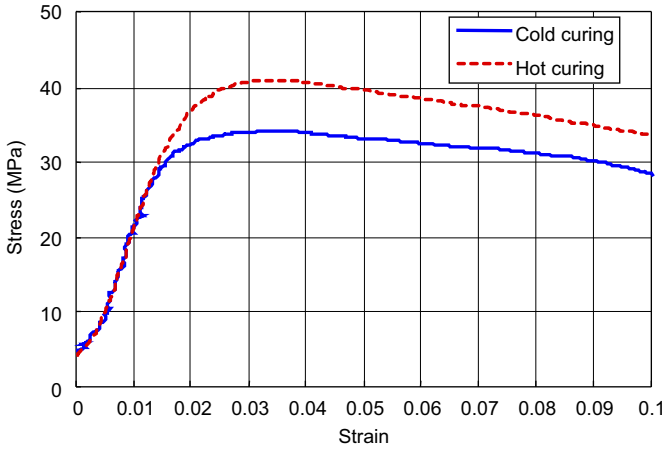

Fig. 9. Comparison of the tensile static tests at $1.0 \times 10^{-3}\,s^{-1}$ for hot and cold curing (curves reported in such a way that the extrapolation of the linear part encounters the origin).

Table 2
Compression tests: equations of the models and of the poly-linear fitting

	Hot curing	Cold curing
Cowper–Symonds	$k = 1 + \left(\frac{\dot{\varepsilon}}{778}\right)^{1/2.66}$	$k = 1 + \left(\frac{\dot{\varepsilon}}{1061}\right)^{1/2.46}$
Johnson–Cook	$k = 1 + 0.146 \ln \frac{\dot{\varepsilon}}{0.101}$	$k = 1 + 0.129 \ln \frac{\dot{\varepsilon}}{0.103}$
Poly-linear fitting	$k = 1.04\dot{\varepsilon}^{0.00594}$, $\dot{\varepsilon} < 0.1\,s^{-1}$	$k = 1.04\dot{\varepsilon}^{0.00492}$, $\dot{\varepsilon} < 0.1\,s^{-1}$
	$k = 1.37\dot{\varepsilon}^{0.0660}$, $0.1\,s^{-1} \leqslant \dot{\varepsilon} \leqslant 1698\,s^{-1}$	$k = 1.36\dot{\varepsilon}^{0.0552}$, $0.1\,s^{-1} \leqslant \dot{\varepsilon} \leqslant 1122\,s^{-1}$
	$k = 0.280\dot{\varepsilon}^{0.281}$, $\dot{\varepsilon} > 1698\,s^{-1}$	$k = 0.378\dot{\varepsilon}^{0.237}$, $\dot{\varepsilon} > 1122\,s^{-1}$

parameters. Three segments have been used to fit the compression data because this choice seems able to reproduce the experimental data behaviour. Table 2 reports, in numerical form, the obtained equations corresponding to the two models and the poly-linear fitting.

4.2. Tensile tests

4.2.1. Tensile static tests

Due to the higher complexity in specimen manufacturing (with respect to the compression case), a lower number of tests have been carried out in total and dynamic tests have been privileged. Fig. 9 shows the engineering stress–strain curves, for the two different types of curing, at the strain-rate $1.0 \times 10^{-3}\,s^{-1}$. This case is the only one that has been considered as static, and such assumption is justified by the observed behaviour of the material (see k factor at the end of Section 4.2.2).

In general terms, under tension the adhesive exhibits lower strength compared to the compression case and a different behaviour after the elastic range. Besides the lower value of the ultimate strain, about 0.1 instead of 0.6 (compare Fig. 9 with Fig. 4), the main aspect is that the decrease of the curves after the peak load is due to cracking, not necking (this can be visually noticed during the tests). The two parts of each broken specimen fit well and the diameter is practically unchanged, since the plastic

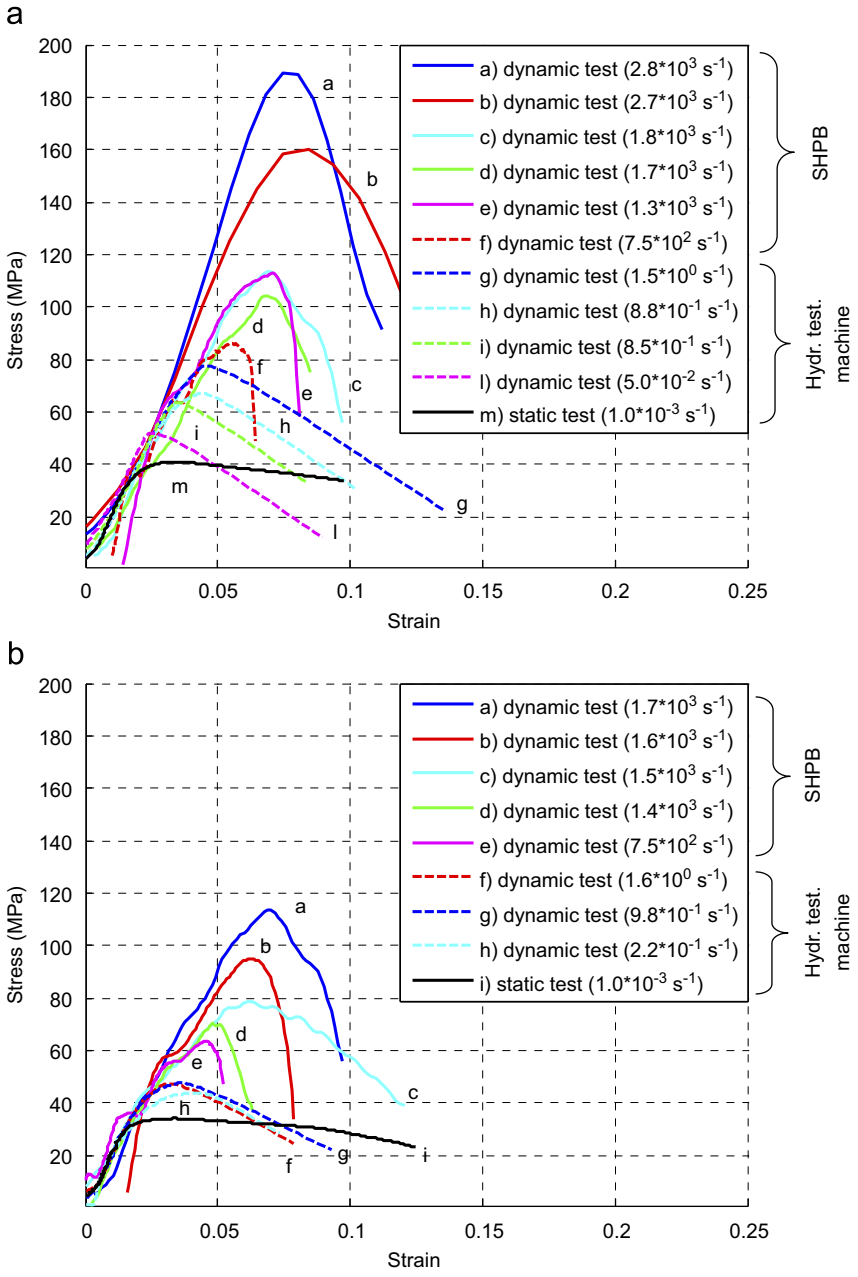

Fig. 10. Summary of the tensile test on specimens: (a) hot cured and (b) cold cured.

deformation is negligible. Thus, the behaviour is substantially brittle.

The hot cured specimens have higher strength than the cold cured ones (15–20%). This phenomenon could be related to the air micro-bubbles in the adhesive that weaken the material: the hot cured specimens are less porous than the cold ones, due to the oven treatment. Furthermore, the structure of the hot cured resin is likely more reticulated.

4.2.2. Tensile dynamic tests

As the compression tests, the tensile dynamics tests have been performed with the servo-hydraulic machine Dartec 100 HA and with the SHPB modified for tensile tests.

Regarding the tests performed with the servo-hydraulic machine, some considerations must be done. As the specimen is loaded by means of the threaded ends, when the crosshead begins to move the specimen, it is immediately loaded, unlike the case of compression (in which a gap was left between upper plate and specimen end). Thus, in the early part of the test, the crosshead has still not achieved the nominal constant speed. Nominal strain-rate values of the order of $10\,s^{-1}$ or greater cannot be obtained because the specimen breaks before the full speed is achieved. As in static conditions, the adhesive exhibits a brittle behaviour at all strain-rate values and the hot cured specimens have higher strength than the cold cured specimens. This effect is more evident in case of high strain-rate tests.

Regarding the test performed with the SHPB, in addition to what is stated previously (Section 2.1), the tensile pulse is distorted due to the great difference in stiffness of the specimen with respect to that of the bars and the threaded geometry. Moreover, since the material is brittle in tension, the reached strain is small and this is an unfavourable condition for the measurements on the SHPB.

Fig. 10 shows, superposed in the same diagram separately for hot and cold curing, the stress–strain curves for the static test at $10^{-3}\,s^{-1}$ and for all dynamic tests. Also in this case the adhesive exhibits lower strength and ultimate strain compared to the compression behaviour (the ultimate strain in Fig. 10 is lower than 0.15, while in Fig. 5 it is in most cases 0.5). It is interesting to note that changing from static to dynamic conditions the plateau of the curve is replaced by a peak, the decrease of the curves is again due to cracking.

Table 3 reports—separately for hot and cold curing—the values of nominal and actual mean strain-rate, the corresponding obtained elastic modulus and the 0.2% proof stress. Regarding the elastic modulus, in addition to what has been remarked for the compression case, it must be noticed that the reported data are affected by an intrinsic problem: the presence of the threaded ends hinders the transverse strain of the short cylindrical portion of the specimen so that in it the stress state is not uniaxial. Thus, the obtained values of E are not accurate and can be regarded as an estimate of the actual uniaxial elastic modulus. In the tested range, it was not possible to notice if

Table 3
Summary of the tensile tests results: (a) hot curing and (b) cold curing

	$\dot{\varepsilon}_{nominal}$ (s^{-1})	$\dot{\varepsilon}_{actual,mean}$ (s^{-1})	E^a (GPa)	$R_{p0.2}$ (MPa)
(a) Hot curing				
Static tests	1.0×10^{-3}	1.00×10^{-3}	2.11	38
Dynamic tests (hydraulic machine)	5.0×10^{-2}	5.10×10^{-2}	2.07	51
	8.5×10^{-1}	8.46×10^{-1}	2.01	59
	8.8×10^{-1}	8.77×10^{-1}	2.10	62
	1.5×10^{0}	1.49×10^{0}	2.07	64
Dynamic tests (SHPB)	7.5×10^{2}	7.60×10^{2}	1.99	80
	1.3×10^{3}	1.32×10^{3}	2.06	107
	1.7×10^{3}	1.68×10^{3}	2.00	97
	1.8×10^{3}	1.81×10^{3}	1.98	105
	2.7×10^{3}	2.71×10^{3}	2.12	149
	2.8×10^{3}	2.82×10^{3}	2.21	179
(b) Cold curing				
Static tests	1.0×10^{-3}	1.0×10^{-3}	2.13	30
Dynamic tests (hydraulic machine)	2.2×10^{-1}	2.19×10^{-1}	2.09	38
	9.8×10^{-1}	9.77×10^{-1}	2.05	42
	1.6×10^{0}	1.62×10^{0}	2.07	42
Dynamic tests (SHPB)	7.5×10^{2}	7.60×10^{2}	1.99	62
	1.4×10^{3}	1.44×10^{3}	1.96	69
	1.5×10^{3}	1.53×10^{3}	1.99	75
	1.6×10^{3}	1.62×10^{3}	1.92	90
	1.7×10^{3}	1.72×10^{3}	1.98	110

[a]Estimate, see comment in the main text.

the strain-rate influences the elastic modulus, neither for hot nor for cold curing. Conversely, as in the compression case, the 0.2% proof stress strongly increases with the strain-rate (three to four times from static to highest tested strain-rate).

In the same way as for the compression tests, it is possible to summarise all tensile tests results in a k–$\dot{\varepsilon}$ diagram. In this case, as the adhesive is brittle, this factor is simply calculated as the ratio of the dynamic (i.e. at the corresponding strain-rate) $R_{p0.2}$ to the static $R_{p0.2}$. The results for the two different types of curing are presented in Fig. 11.

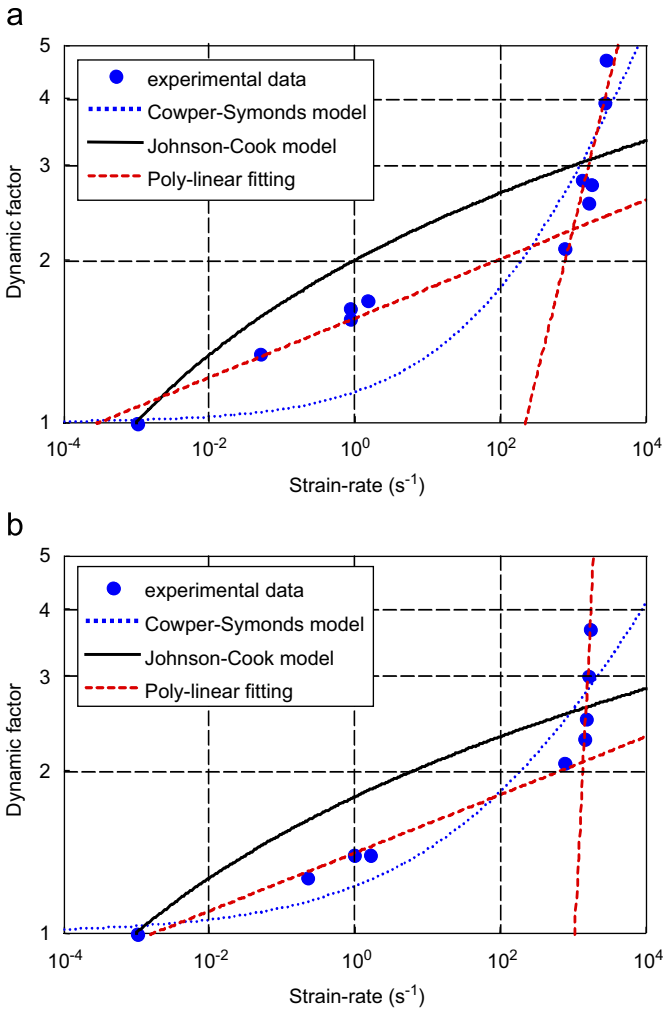

Fig. 11. Dynamic scale factor for specimens: (a) hot cured and (b) cold cured.

Even if the results of tensile tests are fewer than those obtained under compression, it is however possible to discuss the applicability of the above-mentioned literature models. The equations for the two models and for the poly-linear fitting (in this case two segments are adequate to reproduce the behaviour) are shown in Table 4. It appears from Fig. 11 that the Johnson–Cook model does not even fit the intermediate part of the diagram (unlike the compression case). The Cowper–Symonds model fits the points at high strain-rate (better in the hot curing case), whereas in the intermediate range it works only for the cold curing case. The poly-linear fitting gives the best approximation in both cases. It can also be noticed that the influence of the strain-rate in the tensile tests appears to be higher than in compression (note that the dynamic factor ranges up to 5 instead of 3 as in the compression case of Fig. 8).

5. Conclusions

The paper has presented a study of the strain-rate effects on the dynamic mechanical behaviour of a bi-component epoxy adhesive for structural bonding (Hysol 9466). In addition to standard room temperature polymerisation, also the effect of curing at high temperature has been tested.

Both tension and compression tests have been performed, by means of a servo-hydraulic testing machine and a SHPB in the strain-rate range 10^{-3}–$10^{3}\,s^{-1}$. The behaviour of the adhesive is brittle under tension and ductile under compression, at all strain-rate values and for both curing methods. Under the same nominal strain-rate, the hot cured samples exhibit slightly higher strength (in some cases even 10–20% for $R_{p0.2}$).

The adhesive is very sensitive to the strain-rate: for instance, in the tested range, $R_{p0.2}$ grows up to three times under compression and up to five times under tension with respect to the static value, for both curing methods.

Regarding the elastic modulus, as discussed previously some practical problems arise in measuring it with both testing facilities that make the measurement inaccurate. The conclusion that can be drawn on the basis of the available data is that in compression there seems to be a limited effect of the strain-rate on the elastic modulus, in tension it is not possible to observe such effect.

The experimental data fitting by means of the classical dynamic behaviour models (Johnson–Cook and Cowper–Symonds), performed separately for tension/compression

Table 4
Tension tests: equations of the models and of the poly-linear fitting

	Hot curing	Cold curing
Cowper–Symonds	$k = 1 + \left(\frac{\dot{\varepsilon}}{200}\right)^{1/2.66}$	$k = 1 + \left(\frac{\dot{\varepsilon}}{200}\right)^{1/3.49}$
Johnson–Cook	$k = 1 + 0.144 \ln \frac{\dot{\varepsilon}}{1.013\times10^{-3}}$	$k = 1 + 0.114 \ln \frac{\dot{\varepsilon}}{1.007\times10^{-3}}$
Poly-linear fitting	$k = 1.56\dot{\varepsilon}^{0.0549}$, $\dot{\varepsilon} \leqslant 1023\,s^{-1}$	$k = 1.41\dot{\varepsilon}^{0.0538}$, $\dot{\varepsilon} \leqslant 1413\,s^{-1}$
	$k = 5.17 \times 10^{-2}\dot{\varepsilon}^{0.548}$, $\dot{\varepsilon} > 1023\,s^{-1}$	$k = 7.82 \times 10^{-9}\dot{\varepsilon}^{2.68}$, $\dot{\varepsilon} > 1413\,s^{-1}$

and hot/cold curing, is not completely satisfactory since the models do not reproduce the behaviour over the tested strain-rate range. For this reason, a poly-linear fitting in a log–log scale k–$\dot{\varepsilon}$ diagram ($k = \sigma_{\text{dynamic}}/\sigma_{\text{static}}$) has been proposed and adopted. This simple fitting is effective in predicting the experimental points and can be used to obtain useful information when specific data are not available.

An aspect which still needs an explanation is the unexpected ''hourglass'' deformed shape assumed by the cylindrical specimens tested under compression at high strain-rate.

Acknowledgement

This research has been carried out in the framework of the PRIN Project (2004–2006) ''Failure criteria and strength calculation of adhesive joints under monotonic loading'', co-financed by the Italian Ministry of University and Research.

References

[1] Adams RD, Harris JA. A critical assessment of the block impact test for measuring the impact strength of adhesive bonds. Int J Adhes Adhes 1996;16(2):61–71.
[2] Martínez MA, Chocron IS, Rodriguez J, Sanchez Galvez V, Sastre LA. Confined compression of elastic adhesives at high rates of strain. Int J Adhes Adhes 1998;18(6):375–83.
[3] Yokoyama T. Experimental determination of impact tensile properties of adhesive butt joints with the split Hopkinson bar. J Strain Anal 2003;38(3):233–45.
[4] Jones N. Structural impact. Cambridge: University Press; 1989.
[5] Johnson W. Impact strength of materials. London: Arnold; 1972.
[6] Kolsky H. Stress waves in solids. New York: Dover Publications; 1963.
[7] Lee OS, Kim MS. Dynamic material property characterization by using split Hopkinson pressure bar (SHPB) technique. Nucl Eng Des 2003;226(2):119–25.
[8] Hou JP, Ruiz C, Trojanowski A. Torsion test soft thermosetting resins at impact strain rate and under quasi-static loading. Mater Sci Eng (A) 2000;283(1/2):181–8.
[9] Ninan L, Tsai J, Sun CT. Use of split Hopkinson pressure bar for testing off-axis composites. Int J Impact Eng 2001;25(3): 291–313.
[10] Chen W, Lu F, Winfree N. High-strain-rate compression behaviour of a rigid polyurethane foam with various densities. Exp Mech 2002;42(1):65–73.
[11] Chen W, Lu F, Cheng M. Tension and compression tests of two polymers under quasi-static and dynamic loading. Polym Test 2002;21(2):113–21.
[12] Bragov AM, Lomunov AK. Methodological aspects of studying dynamic material properties using the Kolsky method. Int J Impact Eng 1995;16(2):321–30.
[13] Tyas A, Watson AJ. An investigation of frequency domain dispersion correction of pressure bar signals. Int J Impact Eng 2001;25(1): 87–101.
[14] Zhao H, Gary G. On the use of SHPB techniques to determine the dynamic behaviour of materials in the range of small strains. Int J Solids Struct 1996;33(23):3363–75.
[15] Zhao H. Material behaviour characterisation using SHPB techniques, tests and simulations. Comp Struct 2003;81(12):1301–10.